Partition Function Zeros in Two-Dimensional Lattice Models of the Polymer Θ-Point

Vladimir Privman* and Douglas A. Kurtze

Department of Physics, Clarkson University, Potsdam, New York 13676.
Received February 21, 1986

ABSTRACT: We report studies of the partition function zeros in lattice models of interacting self-avoiding walks on the triangular and square lattices. The complex Boltzmann factor-plane zeros show a pattern similar to isotropic lattice spin models. For increasing length of the walks, zeros approach the real axis along a unique locus at the point which can be identified with the "tricritical" singularity, particularly by its location, which is consistent with the Θ-point values found in other numerical studies.

We report studies of the partition function zeros in the self-avoiding walk (SAW) model with nearest-neighbor bond interactions on the square (SQ) and triangular (TR) lattices. This lattice model[1] is believed to have a "tricritical" Θ-point transition.[2,3] Let $c(N,B)$ denote the number of N-step SAW having exactly B nearest-neighbor-site pairs. The partition function for fixed N is defined by

$$Z_N \equiv \sum_B c(N,B)\epsilon^{B-N} \tag{1}$$

where B runs from N to some N-dependent maximum value. The Boltzmann factor $\epsilon > 0$ is assigned per each nearest-neighbor bond contact in excess of the N bonds of the walk itself. It is expected that as $N \to \infty$, thermodynamic quantities become singular at the Θ-point value, $\epsilon_t > 1$. For $0 < \epsilon < \epsilon_t$, the swollen, proper SAW behavior is anticipated. For $\epsilon > \epsilon_t$, the chains would be collapsed, globular. Near the borderline value, ϵ_t, "tricritical" scaling forms have been proposed[2,3] and substantiated by several field-theoretical epsilon-expansion studies.[4-7]

Numerical efforts to verify the theoretical picture have encountered technical difficulties. Since $d = 3$ is the upper critical dimension,[2] logarithmic factors complicate $d = 3$ scaling behaviors. Monte Carlo (MC) studies seem more or less consistent with the theory: see ref 8–10 and literature cited therein. However, series analyses by Rapaport[11] generally contradicted the "tricritical" theory: he found no exponent universality in the SAW and the collapsed regimes. More recently, attention has turned to the two-dimensional systems, which have no "logarithmic" complications. The interest in the physics of the Θ-point in $d = 2$ is more than academic: $d = 2$ polymeric systems in the semicollapsed regime have been realized and studied experimentally.[12-15] It seems, however, that the experimental data available to date do not fit well within the "tricritical" theoretical picture. Numerical MC[16-18] and transfer matrix[19] studies of the SQ-lattice model of interacting SAW described above *are* generally consistent with tricritical scaling predictions. However, the exponent estimates[18,19] obtained by these techniques and also by series analysis methods[20,21] are rather spread and inconsistent with some of the experimental[12] or analytic[22] values.

Our study of the zeros in the complex-ϵ plane of the partition function, $Z_N(\epsilon)$, is intended mainly to establish that their pattern is of a typical form observed for several *isotropic* lattice spin models with a *unique* transition, in the complex temperature plane: see ref 23–29 and literature cited therein. For a review of the Yang–Lee zeros in the complex-H plane, see ref 30 and 31. For anisotropic models, the pattern is distinctively different.[32,33] For the interacting SAW model in *three* dimensions, Rapaport[11] calculated location of zeros but could not draw definite conclusions from their N dependence. However, these complex-plane sequences were far the most regular set of approximants that he[11] calculated. We find, in $d = 2$, that the partition function zeros behave much more smoothly than other sequences of approximants to various quantities used in ref 20 and 21. The zeros can be used to estimate ϵ_t. Unfortunately, accurate estimation of other, *universal* critical-point quantities, which is theoretically possible,[28] seems unfeasible with the existing data.

Table I
SQ-Lattice $N = 21$ Step SAW by Their Bond Content

$B - N$	$c(N,B)/4$	$B - N$	$c(N,B)/4$
0	39 504 435	8	10 792 706
1	91 512 966	9	4 893 520
2	120 863 206	10	1 986 952
3	115 919 582	11	756 634
4	92 235 318	12	239 288
5	63 319 470	13	23 168
6	38 842 204		
7	21 312 058		

The values of $c(N,B;\mathrm{SQ})$ are listed in ref 20 for $N \leq 20$, while $c(N,B;\mathrm{TR})$ have been enumerated[21] to order $N \leq 16$. We generated the SQ-lattice data to order 21: in Table I we list $c(21,B;\mathrm{SQ})$. (We actually obtained $c(\mathrm{SQ})$ for all $N \leq 21$. We used these computer-generated values, checking only a few representative ones against ref 20.) Generally[21] the TR-lattice data provide better approximant sequences, in view of the presence of strong even–odd oscillations in the SQ-lattice results. The value of $\epsilon_t(\mathrm{TR})$ has been estimated:[21]

$$\epsilon_t(\mathrm{TR}) = 1.5 \pm 0.1 \tag{2}$$

For $\epsilon_t(\mathrm{SQ})$, the phenomenological renormalization estimate[19] $\epsilon_t(\mathrm{SQ}) = 2.02 \pm 0.04$, the MC range[17] $\epsilon_t(\mathrm{SQ}) = 2.15 \pm 0.075$, and the series analysis suggestion[20] $\epsilon_t(\mathrm{SQ}) \sim 2.1$ are partially inconsistent. We will assume for reference the range

$$1.98 < \epsilon_t(\mathrm{SQ}) < 2.22 \tag{3}$$

Complex zeros of $Z_{16}(\epsilon;\mathrm{TR})$ are plotted in Figure 1, where we use the notation

$$\epsilon = x + iy \tag{4}$$

The pattern here is very typical for all $N \leq 16$ and also for the SQ lattice. The $x \equiv \mathrm{Re}\,(\epsilon) > 0$ ray is always free from zeros since $c(N,B) > 0$. For given N, a majority of zeros form a claw-shaped structure enclosing the origin of the ϵ plane. The claw "closes" on the part of the real-ϵ axis between $x \sim -1$ and a point which, theoretically, must be at $x = \epsilon_t > 1$. The two complex conjugate arms which trap part of the real axis "grow" as N increases. There is, however, a definite locus which remains well away from

0024-9297/86/2219-2377$01.50/0

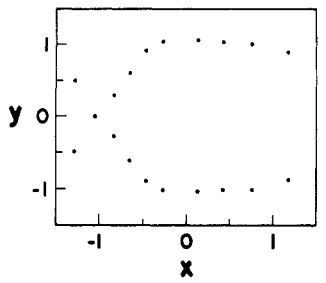

Figure 1. Zeros of $Z_{16}(\epsilon)$ for the triangular lattice. Additional real zero at $\epsilon \simeq -2.97$ is not shown. (Here $\epsilon = x + iy$.)

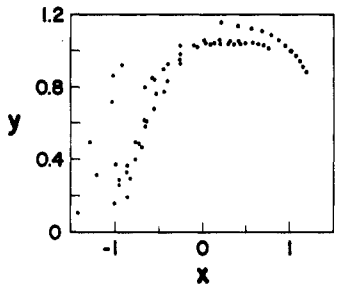

Figure 2. All the $N = 5, ..., 16$ zeros of $Z_N(\epsilon;\mathrm{TR})$ satisfying $x > -1.5$, $y > 0$.

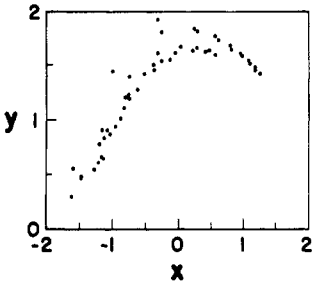

Figure 3. All the $N = 6, ..., 21$ zeros of $Z_N(\epsilon;\mathrm{SQ})$ satisfying $x > -2$, $y > 0$.

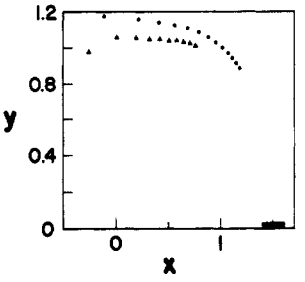

Figure 4. Rightmost (●) and next-to-rightmost (▲) zeros of $Z_N(\epsilon;\mathrm{TR})$ for $N \leq 16$ (only zeros having $x > -0.5$ are displayed). The x coordinates increase monotonically with N within each sequence. The range of eq 2 is indicated on the real axis.

the real-ϵ axis for positive $x < \epsilon_t$. To see that the trapping occurs at the unique point $x = \epsilon_t$, let us first plot in Figure 2 those zeros of $Z_N(\epsilon;\mathrm{TR})$ for $N = 5, ..., 16$ that satisfy $x > -1.5$, $y > 0$. All the $x > -2$, $y > 0$ zeros of $Z_N(\epsilon;\mathrm{SQ})$ for $N = 6, ..., 21$ are shown in Figure 3. Indeed, the distribution of zeros in Figures 2 and 3 shows no tendency to approach the $x > 0$ ray, except perhaps by its rightmost end. This pattern is typical for isotropic spin–lattice models with a unique singularity point.

From now on, we concentrate on the rightmost zero (maximal x) and the one next to it (next-to-maximal x) for each N. We will analyze the trend in x and y of these zeros as N increases. The location of this subset of zeros is shown in Figures 4 and 5 for the TR and the SQ lattices, respectively. By using Figures 4 and 5, one can also easily

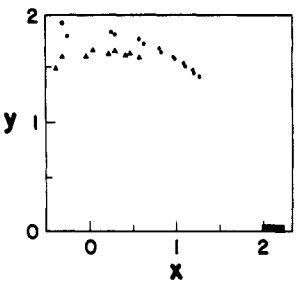

Figure 5. Same as in Figure 4 but for the square lattice. Here $N \leq 21$, and the range marked on the real axis is that of eq 3.

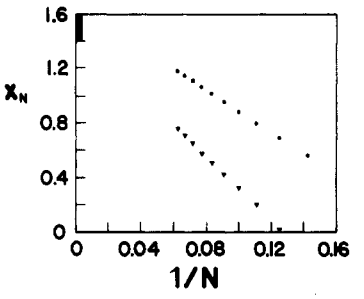

Figure 6. Rightmost (●) and next-to-rightmost (▼) TR-lattice zero real parts, x_N, for $N \leq 16$. Only $x > 0$ points are kept. The range of eq 2 is marked on the x axis.

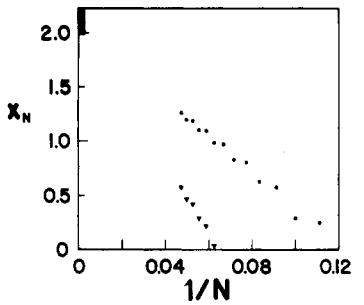

Figure 7. Same as in Figure 6 but for the SQ-lattice with $N \leq 21$. The x range marked is that of eq 3.

identify these sequences of zeros in Figures 2 and 3. The TR-lattice zeros, shown in Figure 4, behave smoothly and seem to close systematically on the real axis at the location consistent with the ϵ_t range of eq 2. The SQ-lattice data (Figure 5) have the usual even–odd oscillations; however, the points do seem to move toward the ϵ_t range of eq 3.

In Figures 6 and 7 we plotted the real parts, x_N, of the rightmost and the following zeros vs. $1/N$ for the TR and the SQ lattice, respectively. The data sequences extrapolate *linearly* to ranges of eq 2 and 3 of ϵ_t. On the other hand, the basic scaling combination at the Θ-point,[2] $N^{\phi}(\epsilon - \epsilon_t)$, entails the crossover exponent ϕ. Extending the scaling ansatz to the complex plane would lead to the convergence laws

$$x_N = \epsilon_t + AN^{-\phi} + ... \tag{5}$$

$$y_N = BN^{-\phi} + ... \tag{6}$$

The crossover exponent has been estimated[21] by series analysis techniques

$$\phi = 0.64 \pm 0.05 \tag{7}$$

This range is consistent with epsilon-expansion[4,6,7] and MC[18] values ($\phi \cong 0.636$ and $\phi \sim 0.6$, respectively). The observed nearly linear convergence of the real parts, x_N, in Figures 6 and 7 suggests that the coefficient A of the leading contribution to $(x_N - \epsilon_t)$ in eq 5 is small or zero for both lattices. To investigate the "scaling" term in the

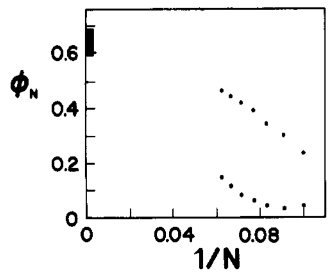

Figure 8. Effective ϕ estimates vs. $1/N$, for the TR lattice ($10 \le N \le 16$). The upper (lower) values correspond to the rightmost (next-to-rightmost) zeros. The range of eq 7 is marked on the ϕ axis.

imaginary part (eq 6), we plotted in Figure 8, the effective ϕ estimates

$$\phi_N = \ln (y_N/y_{N-1})/\ln [(N-1)/N] \qquad (8)$$

vs. $1/N$, for the TR lattice. The values for $N \le 16$ are below 0.64, but their trend in Figure 8 is consistent with them extrapolating toward the range of eq 7 as $N \to \infty$. Study of the SQ-lattice data with $N - 1$ replaced by $N - 2$ in eq 8 produced irregular sequences (all $\phi_N < 0.64$ for $N \le 21$) which, however, show an upward trend similar to the TR-lattice results.

Having an *infinite-slope* locus is not inconsistent with the trend in Figures 4 and 5. By the general considerations of ref 28, the 90° angle implies equal specific heat divergence amplitudes below and above the ϵ_t. The available data, however, are not sufficient to conclusively substantiate this possibility.

In summary, our study of the partition function zeros in the $d = 2$ Θ-point lattice model provides a convincing indication of the existence of a unique transition point at the location consistent with that found in other, "real-axis" numerical studies.

Acknowledgment. We acknowledge instructive discussions with Professor L. S. Schulman.

References and Notes

(1) Fisher, M. E.; Hiley, B. J. *J. Chem. Phys.* **1961**, *34*, 1253.
(2) de Gennes, P.-G. *J. Phys., Lett.* **1975**, *36*, L55.
(3) de Gennes, P.-G. *Scaling Concepts in Polymer Physics*; Cornell University: Ithaca, NY, 1979.
(4) Stephen, M. J. *Phys. Lett. A* **1975**, *53A*, 363.
(5) Kholodenko, A. L.; Freed, K. F. *J. Chem. Phys.* **1984**, *80*, 900; *J. Phys. A: Math. Gen.* **1984**, *A17*, 2703.
(6) Cherayil, B. J.; Douglas, J. F.; Freed, K. F. *J. Chem. Phys.* **1985**, *83*, 5293; *Macromolecules* **1985**, *18*, 2455.
(7) Duplantier, B. *J. Phys. (Les Ulis, Fr.)* **1982**, *43*, 991; Saclay Preprints SPhT/85/153 and SPhT/86/004.
(8) Kremer, K.; Baumgartner, A.; Binder, K. *J. Phys. A: Math. Gen.* **1981**, *A15*, 2879.
(9) Webman, I.; Lebowitz, J. L.; Kalos, M. H. *Macromolecules* **1981**, *14*, 1495.
(10) Bishop, M.; Michels, J. P. J. *J. Chem. Phys.* **1986**, *84*, 447.
(11) Rapaport, D. C. *Macromolecules* **1974**, *7*, 64; *Phys. Lett. A* **1974**, *48A*, 339; *J. Phys. A: Math. Gen.* **1976**, *A9*, 1521; **1977**, *A10*, 637.
(12) Vilanove, R.; Rondelez, F. *Phys. Rev. Lett.* **1980**, *45*, 1502.
(13) Takahashi, A.; Yoshida, A.; Kawaguchi, M. *Macromolecules* **1982**, *15*, 1196; **1983**, *16*, 956.
(14) Kawaguchi, M.; Komatsu, S.; Matsuzumi, M.; Takahashi, A. *J. Colloid Interface Sci.* **1984**, *102*, 356.
(15) Granick, S. *Macromolecules* **1985**, *18*, 1597.
(16) Tobochnik, J.; Webman, I.; Lebowitz, J. L.; Kalos, M. H. *Macromolecules* **1982**, *15*, 549.
(17) Baumgartner, A. *J. Phys. (Les Ulis, Fr.)* **1982**, *43*, 1407.
(18) Birshtein, T. M.; Buldyrev, S. V.; Elyashevitch, A. M. *Polymer* **1985**, *26*, 1814.
(19) Derrida, B.; Saleur, H. *J. Phys. A: Math. Gen.* **1985**, *A18*, L1075.
(20) Ishinabe, T. *J. Phys. A: Math. Gen.* **1985**, *A18*, 3181.
(21) Privman, V. *J. Phys. A: Math. Gen.*, in press.
(22) Coniglio, A.; Jan, N.; Majid, I.; Stanley, H. E. Boston University Preprint, 1985.
(23) Fisher, M. E. In *Lect. Theor. Phys.* **1965**, *12C*, 1.
(24) Jones, G. L. *J. Math. Phys.* **1966**, *7*, 2000.
(25) Abe, R. *Prog. Theor. Phys.* **1967**, *37*, 1070.
(26) Abe, Y.; Katsura, S. *Prog. Theor. Phys.* **1970**, *43*, 1402.
(27) Ono, S.; Karaki, Y.; Suzuki, M.; Kawabata, C. *J. Phys. Soc. Jpn.* **1968**, *25*, 54.
(28) Itzykson, C.; Pearson, R. B.; Zuber, J. B. *Nucl. Phys. B.* **1983**, *B220* [FS8], 415.
(29) Giacomini, H. J. *Phys. Lett. A* **1986**, *115*, 13.
(30) Kurtze, D. A. Cornell University Report MSC 4184 (unpublished).
(31) Fisher, M. E. *Prog. Theor. Phys., Suppl.* **1980**, *69*, 14.
(32) van Saarloos, W.; Kurtze, D. A. *J. Phys. A: Math. Gen.* **1984**, *A17*, 1301.
(33) Stephenson, J.; Couzens, R. *Physica A: (Amsterdam)* **1984**, *129A*, 201.

^{13}C CP/MAS NMR Study of the Polypivalolactone Polymorphs

R. P. Veregin and C. A. Fyfe*

Department of Chemistry and Biochemistry, Guelph–Waterloo Centre for Graduate Work in Chemistry, University of Guelph, Guelph, Ontario, N1G 2W2 Canada

R. H. Marchessault*

Xerox Research Centre of Canada, 2660 Speakman Drive, Mississauga, Ontario, L5K 2L1 Canada.

Received March 11, 1986

ABSTRACT: High-resolution ^{13}C CP/MAS NMR spectra have been obtained for the α, β, and γ polymorphs of polypivalolactone, providing information on their molecular conformation in the solid state. The ^{13}C CP/MAS NMR spectra of the α and γ forms are identical, suggesting that these forms have the same molecular conformation. A characteristic 1:1 doublet is observed for the two chemically "equivalent" methyl carbons, in agreement with the well-established 2_1-helical conformation of the polymer chain in the α form. In contrast, the ^{13}C CP/MAS NMR spectrum of the β form is different from that of the α and γ forms and shows a single peak for the two methyl carbons. The spectrum of the β form is consistent with a planar zigzag molecular conformation for this polymorph.

Introduction

Polypivalolactone (PPL) is the prototype in the series of synthetic α,α-disubstituted polyesters with the general formula

$$-(CH_2CR_1R_2COO)_n-$$
I

where R_1 and R_2 represent various aliphatic substituents. The initial synthesis of these materials by Thiebaut and

